

# Binding and Selectivity of Essential Amino Acid Guests to the Inverted Cucurbit[7]uril Host

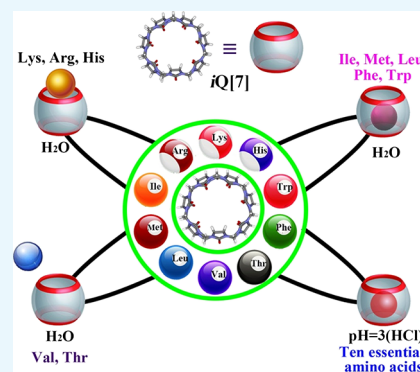
Zhong-Zheng Gao,<sup>†</sup> Jing-Lan Kan,<sup>‡</sup> Li-Xia Chen,<sup>†</sup> Dong Bai,<sup>†</sup> Hai-Yan Wang,<sup>†</sup> Zhu Tao,<sup>†</sup> and Xin Xiao<sup>\*,†</sup>

<sup>†</sup>Key Laboratory of Macrocyclic and Supramolecular Chemistry of Guizhou Province, Guizhou University, Guiyang 550025, P. R. China

<sup>‡</sup>College of Chemistry, Chemical Engineering and Materials Science, Collaborative Innovation Center of Functionalized Probes for Chemical Imaging in Universities of Shandong, Key Laboratory of Molecular and Nano Probes, Ministry of Education, Shandong Normal University, Jinan 250014, P. R. China

## S Supporting Information

**ABSTRACT:** Interactions between inverted cucurbit[7]uril (iQ[7]) and essential amino acids have been studied at pH = 7.0 by <sup>1</sup>H NMR spectroscopy, electronic absorption spectroscopy, isothermal titration calorimetry, and mass spectrometry. The interactions can be divided into three binding types at pH = 7.0. Experimental results from the present study showed that the host displays a strong binding to the aromatic amino acids, Trp and Phe, and the guests of Lys, Arg, and His lie outside the cavity portal of the host. Meanwhile, the alkyl moieties of the guests Met, Leu, and Ile were accommodated within the cavity of iQ[7], but there was no significant interaction between iQ[7] and Thr or Val. The complexation behavior of iQ[7] with essential amino acids was explored at pH = 3, and the binding of Lys, Arg, and His revealed an unexpected behavior, with their side chains located in the cavity of iQ[7], whereas those of the aromatic Trp and Phe were deeper within the iQ[7] cavity. The alkyl side chains of the guests Met, Leu, Ile, Thr, and Val were also located inside the iQ[7] cavity and formed the host–guest complexes.



## INTRODUCTION

In recent years, molecular recognition in biomolecules has attracted considerable attention,<sup>1–4</sup> especially regarding amino acids and aromatic peptides. As the building blocks of proteins, amino acids are essential components of life processes and play critical roles in metabolism growth and development. A lack of any essential amino acids can lead to an abnormal physiological function and eventually to diseases such as nutritional imbalances, Alzheimer's, and pancreatitis.

Research on amino acid and aromatic peptide complexation and recognition by cyclodextrins,<sup>5</sup> calixarenes,<sup>6</sup> pillararenes,<sup>7</sup> and other macrocyclic receptors has been reported. The novel family of macrocycles, cucurbit[*n*]urils (Q[*n*]s, where *n* = 5–8, 10, and 13–15),<sup>8–12</sup> can selectively accommodate and interact with various organic molecules. Several examples of interactions of amino acids with different members of the cucurbit[*n*]urils (Q[*n*]s)<sup>13–18</sup> have been described. Thuéry built chiral assemblies L-Cys-lanthanide–Q[6] complexes using L-cysteine as a chiral linker;<sup>19a</sup> Gamal-Eldin's work on the selective molecular recognition of methylated lysines and arginines by Q[7] had been reported;<sup>19b</sup> and supramolecular structures of tryptophan with Q[6] showed a very interesting and peculiar structure.<sup>20</sup> Kim et al. explored the specific high-affinity binding of Q[7] to amino acids (Lys, Arg, and His and Phe, Tyr, and Trp) in water.<sup>21</sup> Urbach and co-workers observed the 1:1 binding of phenylalanine derivatives to Q[7] and the binding of

aromatic amino acids to Q[8].<sup>22</sup> Nau and co-workers did some work of monitoring of amino acids based on self-assembly.<sup>23</sup>

Scherman's group reported the first example of the recognition of a selected amino acid epitope within a protein by Q[8] complexation.<sup>24</sup> Isaacs's group obtained "turn-on" fluorescent sensors for amino acids using fluorescent cucurbituril derivatives.<sup>25</sup> In 2006 and 2016, our group reported supramolecular receptors for the detection and recognition of amino acids by TMeQ[6],<sup>26</sup> Q[7, 8],<sup>27</sup> and twisted cucurbit[14]uril.<sup>28</sup> This area has seen a large expansion in the number of publications on the binding of amino acids.

In 2005, Isaacs and Kim reported the isolation, characterization, and recognition properties of inverted cucurbit[*n*]urils (iQ[*n*]s, where *n* = 6 and 7),<sup>29</sup> and some related properties of iQ[*n*]s were also described.<sup>30–32</sup> However, to date, few reports have focused on the newest member of the Q[*n*]s, iQ[7]. Our group studied the coordination chemistry of an iQ[7] with a series of metal ions.<sup>33–35</sup> To investigate the host–guest chemistry of the iQ[7], we investigated the binding interaction of an inverted cucurbit[7]uril with  $\alpha,\omega$ -alkyldiammonium guests<sup>36</sup> and 4,4'-bipyridine derivatives.<sup>37,38</sup> In a continuation of this research, herein, we explored the binding of essential

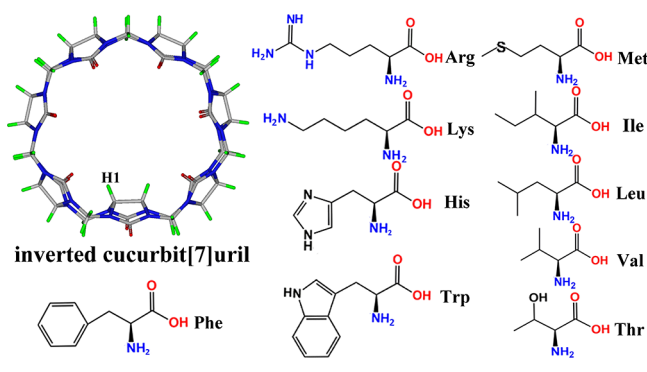
Received: June 16, 2017

Accepted: August 24, 2017

Published: September 8, 2017

amino acids to the iQ[7] host to expand our knowledge of the supermolecular chemistry of iQ[n]s. We studied the binding interactions of iQ[7] with 10 essential amino acids (Scheme 1)

**Scheme 1. Structures of iQ[7] and Essential Amino Acids Investigated in This Work**



in buffered solution by  $^1\text{H}$  NMR spectroscopy, isothermal titration calorimetry (ITC), and matrix-assisted laser desorption ionization time-of-flight mass spectrometry (MALDI-TOF MS). Meanwhile, we also characterized the interaction between iQ[7] and basic amino acids at  $\text{pD} = 3$  by  $^1\text{H}$  NMR spectroscopy. The experimental results provide new insights into the interactions of amino acids and iQ[7].

## RESULTS AND DISCUSSION

**NMR Spectroscopy.** The complexation of iQ[7] with essential L- $\alpha$ -amino acids was first examined by  $^1\text{H}$  NMR spectroscopy of host–guest mixtures. Figure 1 shows the  $^1\text{H}$  NMR spectra of Lys recorded in the absence and presence of approximately 1.0 equiv of the host in  $\text{D}_2\text{O}$ , and  $\text{D}_2\text{O}$  was adjusted to  $\text{pD} = 7.0$  with sodium phosphate. In the presence of iQ[7], the peaks for all methylene protons of Lys display a substantial downfield shift compared with those of the free guest, indicating that all methylene protons interact with the

carbonyl groups of iQ[7]. It has been reported that the  $^1\text{H}$  NMR peaks of the guest protons inside the low-polarizability cavity of Q[n] shift upfield, and interactions with the carbonyl oxygen molecules of Q[n] result in downfield shifts owing to the deshielding of the protons.<sup>21,39,40</sup> Additionally, the signal corresponding to the  $\alpha$ -proton of the amino acid ( $\text{H}_\alpha$ ) is shifted downfield ( $\Delta\delta = 0.37$  ppm). This indicates that the guest is located just outside the portal of the host.

Similar iQ[7] complexation-induced  $^1\text{H}$  NMR changes (downfield shifts and peak splitting) were observed for another two essential amino acids, Arg and His, indicating similar binding modes. The results of titration  $^1\text{H}$  NMR spectroscopy obtained using a fixed amount of iQ[7] and various equivalents of Arg are shown in Figure S1. The side-chain proton ( $\text{H}_\beta$  and  $\text{H}_\gamma$ ) signals for Arg showed a downfield shift of 0.04 and 0.18 ppm, respectively, and the signal for the proton  $\text{H}_\alpha$  showed a downfield shift of 0.29 ppm when the iQ[7]–Arg ratio reached 1:1.02. As shown in Figure S2, the imidazole proton signal of His is shifted downfield compared to that of the free guest, as are the peaks for methylene protons  $\text{H}_\beta$  and  $\text{H}_\alpha$ .

This may reflect the fact that Arg and His lie outside the portal of the host, unlike the interaction of Q[7] with Lys and Arg.<sup>21</sup> The possible reason leading to the difference lies in the smaller cavity of iQ[7] which contains a single inverted glycoluril unit.

The binding behavior of iQ[7] with the aromatic amino acids Trp and Phe clearly departs from our observations with Lys, Arg, and His. As shown in Figure 2, all aromatic protons ( $\text{H}_\gamma$ – $\text{H}_\eta$ ) of Trp move upfield considerably and are broadened compared with those of the free guest as a consequence of inclusion-induced shielding effects. This indicated that they were averaged signals of the free and bound guest molecules due to a rapid exchange rate of binding and release on the NMR time scale. Meanwhile, one of the  $\text{CH}_2$  protons of Trp is moved upfield, which indicates that it is located inside the cavity. By contrast, the proton  $\text{H}_\alpha$  of Trp moved downfield by 0.07 ppm when the iQ[7]–Trp ratio reached 1:1.05, which indicates that it is located outside the cavity. It is noted that the

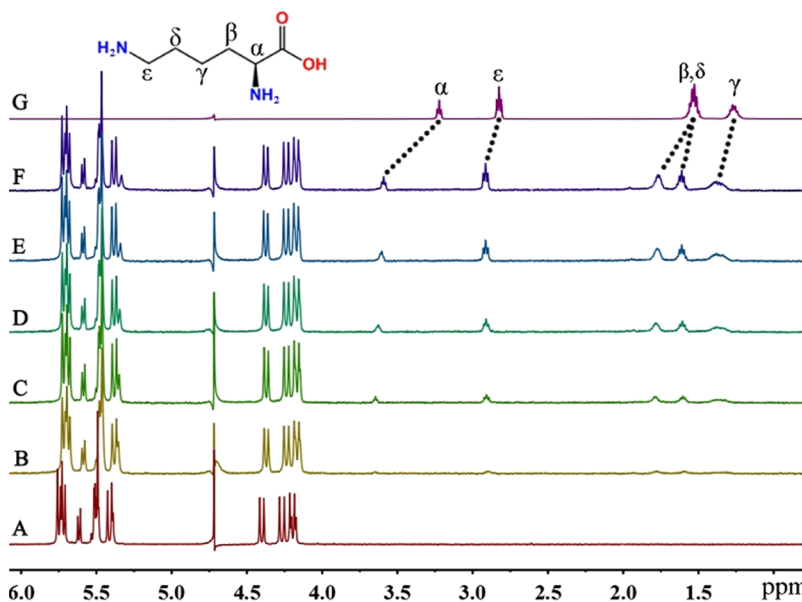


**Figure 1.**  $^1\text{H}$  NMR spectra (400 MHz,  $\text{pD} = 7.0$ ) of iQ[7] in the absence (A) and presence of 0.15 (B), 0.40 (C), 0.70 (D), 0.82 (E), and 1.02 (F) equiv of Lys and free guest Lys (G) at 20  $^\circ\text{C}$ .

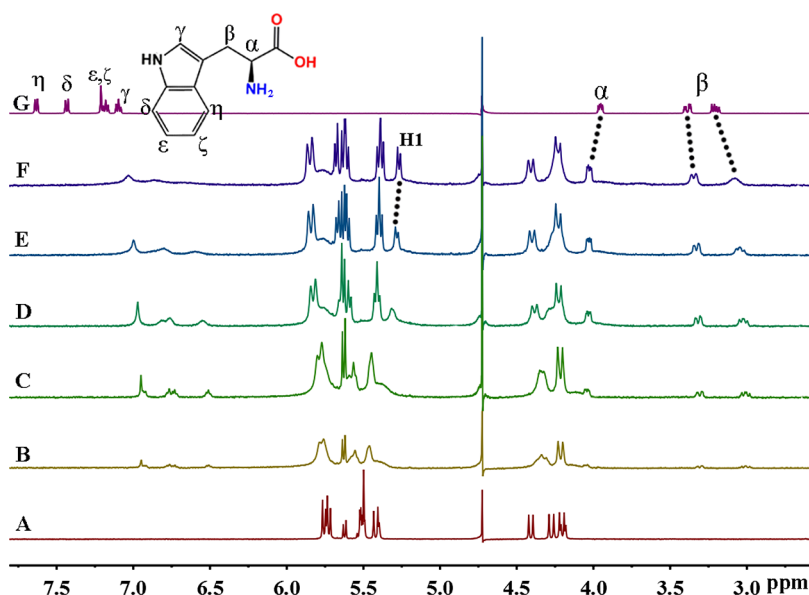


**Figure 2.**  $^1\text{H}$  NMR spectra (400 MHz, pD = 7.0) of iQ[7] in the absence (A) and presence of 0.18 (B), 0.40 (C), 0.64 (D), 0.85 (E), and 1.05 (F) equiv of Trp and free guest Trp (G) at 20  $^\circ\text{C}$ .

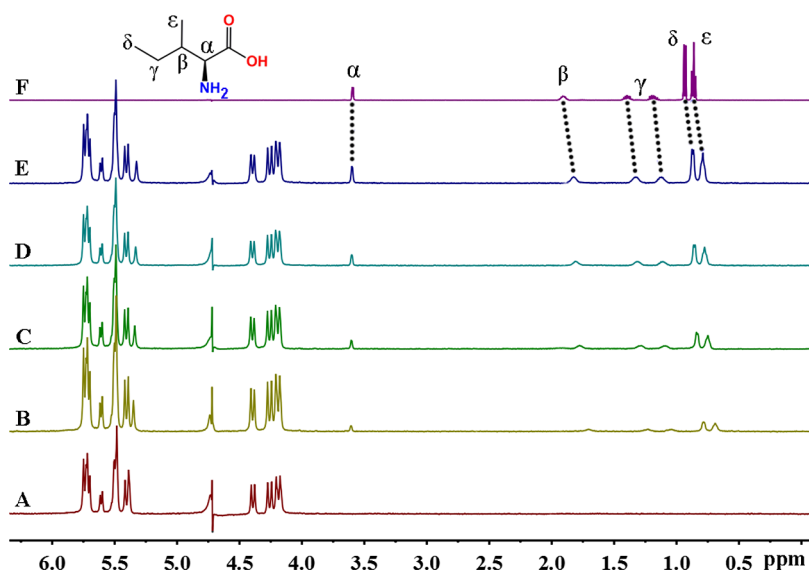


**Figure 3.**  $^1\text{H}$  NMR spectra (400 MHz, pD = 7.0) of iQ[7] in the absence (A) and presence of 0.45 (B), 0.68 (C), 0.85 (D), and 1.05 (E) equiv of Ile and free guest Ile (F) at 20  $^\circ\text{C}$ .

two methine protons (H1 on Scheme 1) of the inverted glycoluril unit in the cavity of iQ[7] were shifted upfield with increasing amounts of Trp, suggesting that Trp also interacts with these methine protons (H1) in the cavity of iQ[7]. These observations suggest that the  $\text{CH}_2$  group and indole moiety of the Trp guest are encapsulated in the cavity of the iQ[7] host. This is also the case for the binding interactions of iQ[7] with Phe; as shown in Figure S3, the aromatic ring protons of Phe are clearly subject to upfield shifts upon binding to iQ[7].

Meanwhile, the signal corresponding to the  $\alpha$ -proton of the bound amino acid ( $\text{H}_\alpha$ ) is shifted obviously downfield ( $\Delta\delta = 0.13$  ppm), similar to the binding interactions of iQ[7] with Trp. This result is consistent with the binding behavior of Q[7] with aromatic amino acids.<sup>21</sup>

The interaction of iQ[7] with Ile could be conveniently monitored by  $^1\text{H}$  NMR. A slight upfield shift of the signals of the protons of the alkyl chain ( $\text{H}_\beta$ – $\text{H}_\delta$ ) and a slight downfield

shift of the signal of the  $\text{H}_\alpha$  were observed upon the addition of iQ[7] (Figure 3), suggesting that there is a weak interaction between iQ[7] and Ile. Similar  $^1\text{H}$  NMR spectra for the interaction of iQ[7] and the guests Leu and Met were also recorded (Figures S4 and S5). This indicates that the alkyl moiety of the guests was accommodated within the cavity of iQ[7] but the interaction is weak. Meanwhile, no obvious shift was observed when mixing the host with the essential amino acids, Val or Thr (Figures S6 and S7).

To compare the binding patterns of the essential amino acids with iQ[7] under different conditions, we also investigated the interactions between the protonated forms of the amino acids and iQ[7] by  $^1\text{H}$  NMR titration at pD = 3. We first studied the binding behavior of three basic amino acids with iQ[7]. A trace amount of the acid was added together with iQ[7] to ensure the formation of the complexes. With 1.0 equiv of Lys, Arg, or His, the proton of the side chains of these amino acids showed

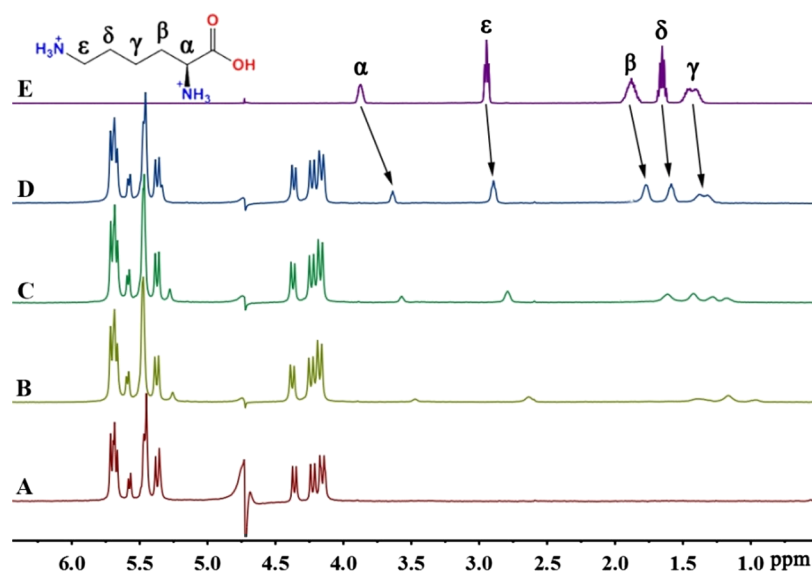


**Figure 4.**  $^1\text{H}$  NMR spectra (400 MHz,  $\text{pD} = 3$ ) of iQ[7] in the absence (A) and presence of 0.35 (B), 0.75 (C), and 1.05 (D) equiv of Lys and free guest Lys (E) at  $20^\circ\text{C}$ .

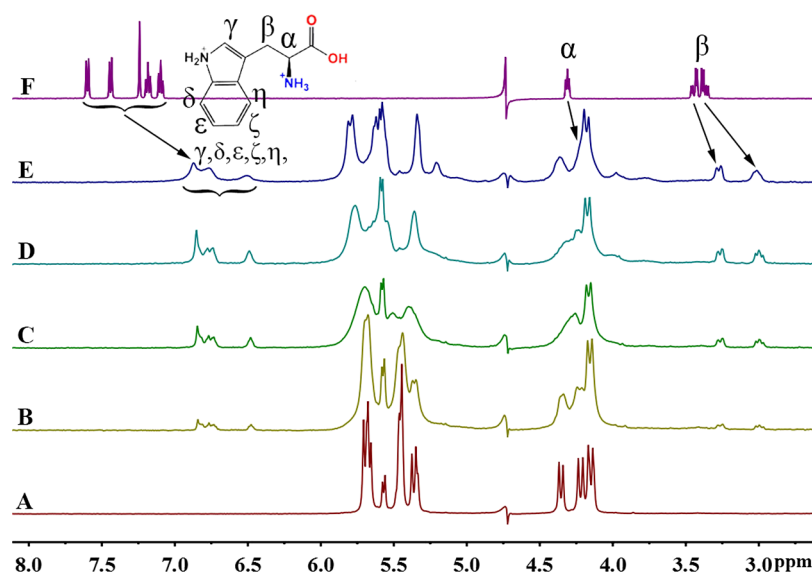


**Figure 5.**  $^1\text{H}$  NMR spectra (400 MHz,  $\text{pD} = 3$ ) of iQ[7] in the absence (A) and presence of 0.35 (B), 0.70 (C), 0.85 (D), and 1.05 (E) equiv of Trp and free guest Trp (F) at  $20^\circ\text{C}$ .

a significant upfield displacement (Figures 4, S8, and S9), indicating the formation of complexes. Lys, Arg, and His showed unexpected changes at  $\text{pD} = 3$  compared with  $\text{D}_2\text{O}$  because  $^1\text{H}$  NMR experiments confirmed that these amino acids formed inclusion complexes with iQ[7]. This change in behavior is likely due to a change in the protonation state.<sup>21</sup> We concluded that the side chains of Lys, Arg, and His were predominantly located in a shielded environment.<sup>21,39,40</sup> This is because the binding to iQ[7] causes His, Lys, and Arg to favor the fully protonated state. As Kim reported before, paying the thermodynamic penalty for the protonation of the carboxylate group is favored over the binding to iQ[7] as the deprotonated form.

For Trp and Phe, the amino groups of the guests remained protonated at  $\text{pD} = 3$ . Next, we investigated the binding interactions of the aromatic amino acids Trp and Phe with iQ[7]. The interaction of Trp with iQ[7] was studied first

(Figure 5), and the results showed that the proton of the indole moiety was shifted upfield, suggesting that the indole moiety of Trp was located inside the cavity, as concluded previously. Upon comparing the differences, it became apparent that the protons  $\text{H}_\alpha$  and  $\text{H}_\beta$  of Trp were shifted upfield, indicating that the methylene and methine groups of the guest were also encapsulated in the iQ[7] cavity. This conclusion was also reached for Phe. As shown in Figure S10, all protons of the benzyl moiety underwent a considerable upfield shift; meanwhile, the  $\text{H}_\alpha$  protons also experienced a small upfield shift. These iQ[7]-induced shift patterns suggested that the benzene ring and alkyl chain moiety of Phe were situated inside the iQ[7] cavity. Overall, the results suggest that Trp and Phe guests were buried deeper within the iQ[7] cavity. This indicates that the aromatic amino acids can maintain their binding affinities reasonably well even if their carboxyl groups

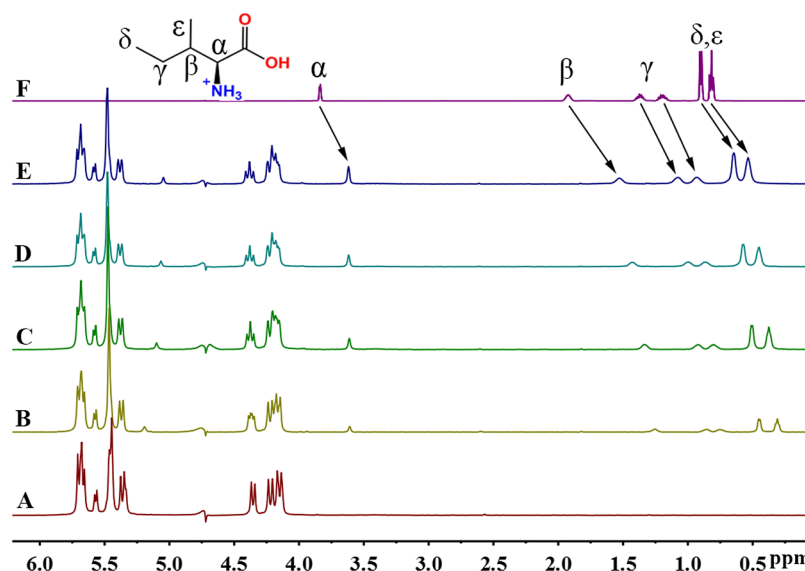


**Figure 6.**  $^1\text{H}$  NMR spectra (400 MHz, pD = 3) of iQ[7] in the absence (A) and presence of 0.30 (B), 0.65 (C), 0.85 (D), and 1.05 (E) equiv of Ile and free guest Ile (F) at 20  $^\circ\text{C}$ .

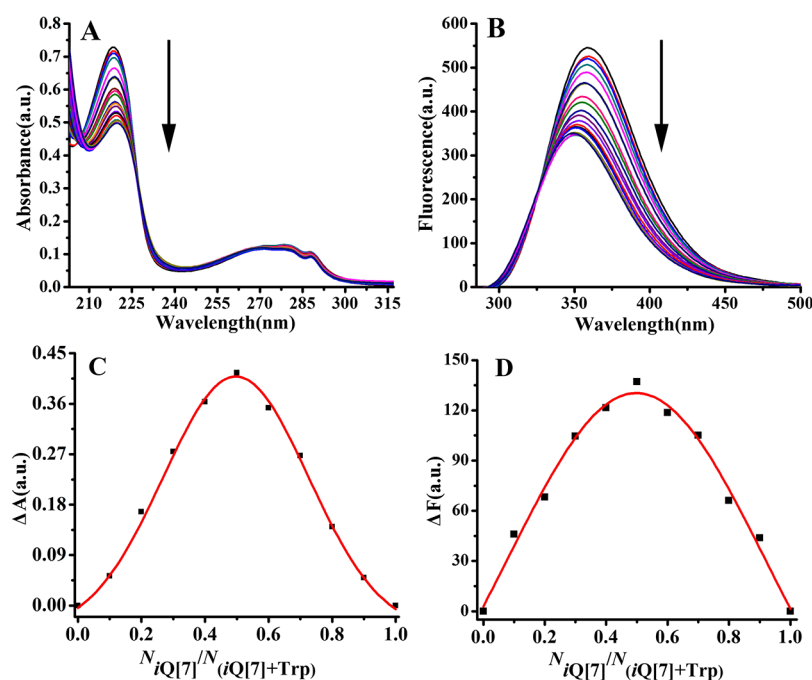


**Figure 7.** Electronic absorption (A) and fluorescence emission spectra (B) of Trp ( $2 \times 10^{-5}$  mol·L $^{-1}$ ) upon the addition of increasing amounts (0, 0.1, 0.2, 0.3, 0.4, 0.5, 0.6, 0.7, 0.8, 0.9, 1.0, 1.1, 1.2, 1.3, 1.4, 1.5, 1.6, 1.7, 1.8, 1.9, and 2.0 equiv) of iQ[7].  $\Delta A$  (C) and  $\Delta F$  (D) vs  $N_{\text{iQ}[7]}/(N_{\text{iQ}[7]} + N_{\text{Trp}})$  plots.

are deprotonated, which is consistent with the results of the binding of Q[7] with aromatic amino acids.

The host–guest interactions of iQ[7] with charged amino acids (Ile, Leu, Met, Val, and Thr) at pD = 3 were also investigated by  $^1\text{H}$  NMR spectroscopy. The  $^1\text{H}$  NMR spectra of Ile and Ile bound to iQ[7] are shown in Figure 6. All protons of the alkyl side chain of Ile were clearly shifted upfield by between 0.23 and 0.41 ppm, indicating burial within the iQ[7] cavity. Similarly, when the amino acids were added to iQ[7] at pD = 3, the alkyl side-chain protons of Leu, Met, Val, and Thr experienced a significant upfield shift, suggesting a deep inclusion in the cavity of iQ[7] due to the formation of inclusion complexes (Figures S11–S14). Upon comparing with

nuclear magnetic titration experiments in  $\text{D}_2\text{O}$ , it became apparent that the alkyl side-chain protons of the guests were shifted upfield, confirming that these four amino acids were more likely to form inclusion complexes at pD = 3. Major binding differences were observed (using NMR spectroscopy) between pD = 7 and 3, which can be explained as a consequence of the different protonation state for the carboxylate group. Upon the protonation of the carboxylate group, the amino acid inclusion into the cucurbituril cavity is favored.

**Ultraviolet–Visible Absorption and Fluorescence Emission Spectra.** The interaction of iQ[7] with Trp was also examined by UV absorbance spectrophotometry and



fluorescence spectroscopy. According to the UV absorption spectroscopic results (Figure 7A), the gradual addition of iQ[7] to Trp in buffered solution (pH = 7) was accompanied by a significant decrease in the intensity at 218 nm and a slight bathochromic shift because of the strong interaction between iQ[7] and Trp. As can be seen in Figure 7B, Trp displayed an emission peak at 366 nm at an excitation wavelength of 269 nm. Successive addition of iQ[7] caused a decrease and a hypsochromic shift from 359 to 350 nm in the fluorescence intensity at 359 nm. These substantial changes in the emission profile further confirm the strong host–guest interaction between iQ[7] and Trp. From the ultraviolet–visible (UV–vis) absorption and fluorescence intensity, the binding constant ( $K_a$ ) for iQ[7]–Trp could be determined to be  $2.32 \times 10^4 \text{ M}^{-1}$  and  $2.68 \times 10^4 \text{ M}^{-1}$ . Furthermore, Job's plots (Figure 7C,D) based on the continuous variation method clearly showed that the UV spectra and fluorescence spectra of Trp fitted well with 1:1 stoichiometry of the host–guest inclusion complexes.

**Isothermal Titration Calorimetry.** To better understand the host–guest interactions between iQ[7] and the 10 essential L- $\alpha$ -amino acids, we carried out at least two ITC experiments at 25 °C in 10 mM sodium phosphate (pH 7.0). Table 1 and

**Table 1. Complex Stability Constant ( $K_a$ ), Enthalpy ( $\Delta H^\circ$ ), Entropy Changes ( $T\Delta S^\circ$ ), and Gibbs Free Energy ( $\Delta G^\circ$ ) for iQ[7]–Guest Interactions in Buffered Solution at pH = 7**

| guest | $K_a (\times 10^4 \text{ M}^{-1})$ | $\Delta H^\circ (\text{kJ/mol})$ | $T\Delta S^\circ (\text{kJ/mol})$ | $\Delta G^\circ (\text{kJ/mol})$ |
|-------|------------------------------------|----------------------------------|-----------------------------------|----------------------------------|
| Lys   | $0.87 \pm 0.15$                    | $-31.2 \pm 14.0$                 | $-4.17$                           | $-27.1$                          |
| Arg   | $1.60 \pm 0.97$                    | $-32.4 \pm 9.55$                 | $-4.23$                           | $-28.2$                          |
| His   | $0.66 \pm 0.13$                    | $-33.8 \pm 11.0$                 | $-7.93$                           | $-25.9$                          |
| Trp   | $2.83 \pm 0.66$                    | $-37.4 \pm 5.71$                 | $-12.0$                           | $-25.4$                          |
| Phe   | $10.7 \pm 0.24$                    | $-37.6 \pm 2.25$                 | $-9.62$                           | $-28.0$                          |

Figures S15 and S16 show the equilibrium association constants ( $K_a$ ) and thermodynamic parameters for iQ[7]–amino acid interaction systems for Lys, Arg, His, Trp, and Phe. The experimental results revealed  $K_a$  values ranging from  $\sim 10^3$  to  $\sim 10^5 \text{ M}^{-1}$  and negative  $\Delta G^\circ$  values ranging from  $-25.4$  to  $-28.2 \text{ kJ/mol}$  for iQ[7]–amino acid interactions. Thus, these L- $\alpha$ -amino acids could effectively bind to the iQ[7] host. However, the amino acids Met, Ile, Leu, Thr, and Val showed no effective interaction with iQ[7] (Figure S17). The revealed  $K_a$  values indicated a strong binding with the aromatic amino acids Trp and Phe, among which iQ[7] binds with Phe with the highest binding affinity, which is consistent with the binding behavior of Q[7] with aromatic amino acids (Table 2).<sup>21,41</sup> The observations can be explained in terms of a combination of ion-dipole and electrostatic interactions between the positively

**Table 2. Complex Stability Constant ( $K_a$ ), Enthalpy ( $\Delta H^\circ$ ), and Entropy Changes ( $T\Delta S^\circ$ ) for Q[7]–Guests**

| guest | $K_a (\text{M}^{-1})$      | $\Delta H^\circ (\text{kJ/mol})$ | $T\Delta S^\circ (\text{kJ/mol})$ |
|-------|----------------------------|----------------------------------|-----------------------------------|
| Lys   | $2.1(\pm 0.7) \times 10^2$ | $-4.4 \pm 0.3$                   | $8.8 \pm 0.3$                     |
| Arg   | <sup>a</sup> not available |                                  |                                   |
|       | <sup>b</sup> $327 \pm 16$  | $-5.0 \pm 0.1$                   | $9.2 \pm 0.1$                     |
| His   | <sup>a</sup> not available |                                  |                                   |
| Trp   | $1.2(\pm 0.1) \times 10^3$ | $-28.9 \pm 0.6$                  | $-11.3 \pm 0.6$                   |
| Phe   | $1.8(\pm 0.5) \times 10^5$ | $-30.5 \pm 2.8$                  | $-0.6 \pm 2.8$                    |

<sup>a</sup>Measured in sodium phosphate buffer at pH = 7.0, ref 21. <sup>b</sup>Measured in sodium phosphate buffer at pH = 6.0, ref 41.

charged side chains of the amino acids and the polar carbonyl groups of iQ[7] and hydrophobic interactions between the aromatic moieties of the amino acids and the macrocyclic cavity. From the  $\Delta H^\circ$  and  $T\Delta S^\circ$  values shown in Table 1, all intermolecular complexation interactions between the iQ[7] host and L- $\alpha$ -amino acids guests appear to be driven by favorable enthalpy changes, accompanied by small negative (unfavorable) entropy changes. According to the NMR data, the interactions between iQ[7] and Met, Ile, and Leu are relatively weak; meanwhile, iQ[7] with Thr and Val shows no interaction. These facts might be a reasonable explanation why the ITC experiments showed no effective interaction of iQ[7] with these amino acids Met, Ile, Leu, Thr, and Val.

**Mass Spectrometry.** We further studied the formation of the inclusion complexes of iQ[7] and guests for 10 of the essential L- $\alpha$ -amino acids by MALDI-TOF MS. In the resultant MALDI-TOF MS spectra (Figure S18), major signals at  $m/z = 1309.012$ ,  $1336.526$ ,  $1317.864$ ,  $1367.793$ ,  $1328.397$ ,  $1294.573$ ,  $1294.498$ , and  $1312.410$  were observed, corresponding to Lys–iQ[7] (calculated 1309.151), Arg–iQ[7] (calculated 1337.164), His–iQ[7] (calculated 1318.118), Trp–iQ[7] (calculated 1367.189), Phe–iQ[7] (calculated 1328.152), Ile–iQ[7] (calculated 1294.136), Leu–iQ[7] (calculated 1294.136), and Met–iQ[7] (calculated 1312.175), respectively. These intense signals provide direct support for the formation of 1:1 stoichiometric host–guest inclusion complexes for these eight amino acids. It is noted that no significant host–guest interaction signals were observed between iQ[7] and Thr or Val in the MS spectra. The results of the mass spectra are consistent with the results from the NMR experiments.

## CONCLUSIONS

We explored the binding interactions between 10 essential L- $\alpha$ -amino acid guests and the iQ[7] host using a variety of characterization methods in buffered solution (pH = 7). The experimental results indicated a strong binding with the aromatic amino acids Trp and Phe, and iQ[7] binds with Phe with the highest binding affinity, which is consistent with the binding behavior of Q[7] with aromatic amino acids. Lys, Arg, and His guests lie outside the portal of the host, whereas the alkyl moieties of Met, Leu, and Ile guests were accommodated within the iQ[7] cavity, and there was no significant interaction between iQ[7] and Thr or Val. Additionally, interactions between the protonated form of Lys, Arg, and His with iQ[7] were also investigated at pH = 3, and unexpectedly, the side chains were located in the cavity of iQ[7] under acidic conditions. Furthermore, the aromatic amino acids Trp and Phe were more deeply buried in the iQ[7] cavity at the lower pH. An upfield chemical shift for the protons of the alkyl side chains of Met, Leu, Ile, Thr, and Val guests indicated that they were located inside the iQ[7] cavity and hence formed host–guest complexes. These results not only enhance our knowledge of the molecular recognition of amino acids but may also be of significance for the design and synthesis of new macrocyclic compounds for biological identification and simulation.

## EXPERIMENTAL SECTION

**Materials and Reagents.** Ten essential L- $\alpha$ -amino acids were purchased from Aldrich. iQ[7] was prepared and purified according to our previously published procedure.<sup>33</sup> All other

reagents were of analytical grade and were used as received. Double-distilled water was used for all experiments.

**Nuclear Magnetic Resonance Measurements.** All  $^1\text{H}$  NMR spectra, including those for titration experiments, were measured on a Varian INOVA-400 NMR spectrometer with  $\text{SiMe}_4$  as an internal reference at  $20^\circ\text{C}$ .  $\text{D}_2\text{O}$  was used as a field-frequency lock, and the observed chemical shifts are reported in parts per million (ppm) relative to that for the internal standard (TMS at 0.0 ppm). The ratio of amino acids versus iQ[7] was calculated by the ratio of their integral areas for special peaks. The concentrations of the amino acids were  $1.0 \times 10^{-4}$  mol/L in the NMR experiments.  $\text{D}_2\text{O}$  was adjusted to  $\text{pD} = 7.0$  with sodium phosphate. The value was verified on a pH meter calibrated with two standard buffer solutions.  $\text{D}_2\text{O}$  was adjusted to  $\text{pD} = 3.0$  with 1 M DCl. The  $\text{pD} = 3$  of the solution was also verified on a calibrated pH meter.

**UV–Vis Absorption and Fluorescence Emission Spectra.** UV–vis absorption spectra of the host–guest complexes were recorded with an Agilent 8453 spectrophotometer at room temperature. Fluorescence spectra measurements were performed on a Varian Cary Eclipse fluorescence spectrophotometer equipped with a xenon discharge lamp at room temperature. The absorption and fluorescence titration experiments were performed as follows:  $200.0\ \mu\text{L}$  of  $1.0 \times 10^{-3}$  mol/L stock solution of Trp and various amounts of  $1.0 \times 10^{-4}$  mol/L iQ[7] aqueous solution were transferred into a 10 mL volumetric flask, and then the volumetric flask was filled to the final volume with distilled water. The pH was adjusted to  $\text{pH} = 7$  with sodium phosphate.

**ITC Measurements.** Microcalorimetric experiments were performed using an isothermal titration calorimeter Nano ITC (TA, USA). The heat evolved was recorded at 298.15 K. The heat of the reaction was corrected for the heat of the dilution of the guest solution determined in separate experiments. All solutions were degassed prior to the titration experiment by sonication. A stock solution ( $1.0 \times 10^{-3}$  mol/L) of amino acids and  $1.0 \times 10^{-4}$  mol/L stock solution of iQ[7] were prepared with 10 mM sodium phosphate ( $\text{pH} = 7.0$ ). A typical ITC titration was carried out by titrating the L- $\alpha$ -amino acid solution ( $\text{pH} = 7$ ,  $1.0 \times 10^{-3}$  mol/L,  $6\ \mu\text{L}$  of aliquots, at 250 s intervals) into an iQ[7] solution. The concentration of iQ[7] in the sample cell (1.3 mL) was  $1.0 \times 10^{-4}$  mol/L at  $\text{pH} = 7$ . Computer simulations (curve fitting) were performed using the Nano ITC analyze software. First points in the ITC data were excluded when fitting the model to acquire the binding constant, enthalpy change, and entropy change.

**MALDI-TOF MS.** MALDI-TOF MS spectra were recorded on a Bruker BIFLEX III ultrahigh-resolution Fourier transform ion cyclotron resonance mass spectrometer with  $\alpha$ -cyano-4-hydroxycinnamic acid as the matrix. The MALDI-TOF experiments were carried out by adding the L- $\alpha$ -amino acid solution ( $1.0 \times 10^{-3}$  mol/L,  $100\ \mu\text{L}$ ) into an iQ[7] solution ( $1.0 \times 10^{-4}$  mol/L, 1.0 mL). The solution concentration was about  $1.0 \times 10^{-4}$  mol/L (L- $\alpha$ -amino acids–iQ[7] = 1:1).

## ■ ASSOCIATED CONTENT

### ● Supporting Information

The Supporting Information is available free of charge on the ACS Publications website at DOI: 10.1021/acsomega.7b00429.

NMR spectra, MALDI-TOF MS spectra of inclusion complexes, and ITC profiles of iQ[7] with guests (PDF)

## ■ AUTHOR INFORMATION

### Corresponding Author

\*E-mail: gyhxxiaoxin@163.com (X.X.).

### ORCID

Xin Xiao: 0000-0001-6432-2875

### Notes

The authors declare no competing financial interest.

## ■ ACKNOWLEDGMENTS

This work was financially supported by the National Natural Science Foundation of China (no. 21561007), the Innovation Program for High-level Talents of Guizhou Province (no. 2016-5657), the Science and Technology Fund of Guizhou Province (no. 2016-1030), and the Scientific Research Foundation of Guizhou University (no. 2015-62).

## ■ REFERENCES

- (1) Joseph, R.; Rao, C. P. Ion and molecular recognition by lower rim 1,3-di-conjugates of calix[4]arene as receptors. *Chem. Rev.* **2011**, *111*, 4658–4702.
- (2) Zheng, B.; Wang, F.; Dong, S.; Huang, F. Supramolecular polymers constructed by crown ether-based molecular recognition. *Chem. Soc. Rev.* **2012**, *41*, 1621–1636.
- (3) (a) Barrow, S. J.; Kasera, S.; Rowland, M. J.; del Barrio, J.; Scherman, O. A. Cucurbituril-Based Molecular Recognition. *Chem. Rev.* **2015**, *115*, 12320–12406. (b) Yu, G.; Jie, K.; Huang, F. Supramolecular Amphiphiles Based on Host–Guest Molecular Recognition Motifs. *Chem. Rev.* **2015**, *115*, 7240–7303. (c) Jie, K.; Zhou, Y.; Yao, Y.; Huang, F. Macrocyclic amphiphiles. *Chem. Soc. Rev.* **2015**, *44*, 3568–3587.
- (4) (a) Ji, X.; Wang, H.; Li, Y.; Xia, D.; Li, H.; Tang, G.; Sessler, J. L.; Huang, F. Controlling amphiphilic copolymer self-assembly morphologies based on macrocycle/anion recognition and nucleotide-induced payload release. *Chem. Sci.* **2016**, *7*, 6006–6014. (b) Yu, G.; Zhou, J.; Shen, J.; Tang, G.; Huang, F. Cationic pillar[6]arene/ATP host–guest recognition: Selectivity, inhibition of ATP hydrolysis, and application in multidrug resistance treatment. *Chem. Sci.* **2016**, *7*, 4073–4078. (c) Zhang, M.; Yan, X.; Huang, F.; Niu, Z.; Gibson, H. W. Stimuli-Responsive Host–Guest Systems Based on the Recognition of Cryptands by Organic Guests. *Acc. Chem. Res.* **2014**, *47*, 1995–2005.
- (5) Saha, S.; Ray, T.; Basak, S.; Roy, M. N. NMR, surface tension and conductivity studies to determine the inclusion mechanism: thermodynamics of host–guest inclusion complexes of natural amino acids in aqueous cyclodextrins. *New J. Chem.* **2016**, *40*, 651–661.
- (6) (a) Yang, F.; Ji, Y.; Guo, H.; Lin, J.; Peng, Q. Calix[4]arene Polyaza Derivatives: Novel Effective Neutral Receptors for Cations and  $\alpha$ -Amino Acids. *Chem. Res. Chin. Univ.* **2006**, *22*, 808–810. (b) Chinta, J. P.; Acharya, A.; Kumar, A.; Rao, C. P. Spectroscopy and Microscopy Studies of the Recognition of Amino Acids and Aggregation of Proteins by Zn(II) Complex of Lower Rim Naphthylidene Conjugate of Calix[4]arene. *J. Phys. Chem. B* **2009**, *113*, 12075–12083.
- (7) Li, C.; Ma, J.; Zhao, L.; Zhang, Y.; Yu, Y.; Shu, X.; Li, J.; Jia, X. Molecular selective binding of basic amino acids by a water-soluble pillar[5]arene. *Chem. Commun.* **2013**, *49*, 1924–1926.
- (8) Freeman, W. A.; Mock, W. L.; Shih, N. Y. Cucurbituril. *J. Am. Chem. Soc.* **1981**, *103*, 7367–7368.
- (9) Kim, J.; Jung, I.-S.; Kim, S.-Y.; Lee, E.; Kang, J.-K.; Sakamoto, S.; Yamaguchi, K.; Kim, K. New Cucurbituril Homologues: Syntheses, Isolation, Characterization, and X-ray Crystal Structures of Cucurbit-[n]uril (n = 5, 7, and 8). *J. Am. Chem. Soc.* **2000**, *122*, 540–541.
- (10) Day, A. I.; Blanch, R. J.; Arnold, A. P.; Lorenzo, S.; Lewis, G. R.; Dance, I. A Cucurbituril-Based Gyroscane: A New Supramolecular Form. *Angew. Chem.* **2002**, *114*, 285–287. DOI: 10.1002/1521-3757(20020118)114:2<285::aid-ange285>3.0.co;2-6; *Angew. Chem.*

*Int. Ed.* **2002**, *41*, 275–277. [10.1002/1521-3773\(20020118\)41:2<275::aid-anie275>3.0.co;2-m](https://doi.org/10.1002/1521-3773(20020118)41:2<275::aid-anie275>3.0.co;2-m)

(11) Cheng, X.-J.; Liang, L.-L.; Chen, K.; Ji, N.-N.; Xiao, X.; Zhang, J.-X.; Zhang, Y.-Q.; Xue, S.-F.; Zhu, Q.-J.; Ni, X.-L.; Tao, Z. Twisted Cucurbit[14]uril. *Angew. Chem., Int. Ed.* **2013**, *52*, 7252–7255.

(12) Li, Q.; Qiu, S.-C.; Zhang, J.; Chen, K.; Huang, Y.; Xiao, X.; Zhang, Y.; Li, F.; Zhang, Y.-Q.; Xue, S.-F.; Zhu, Q.-J.; Tao, Z.; Lindoy, L. F.; Wei, G. Twisted Cucurbit[n]urils. *Org. Lett.* **2016**, *18*, 4020–4023.

(13) Buschmann, H.-J.; Schollmeyer, E.; Mutihac, L. The formation of amino acid and dipeptide complexes with  $\alpha$ -cyclodextrin and cucurbit[6]uril in aqueous solutions studied by titration calorimetry. *Thermochim. Acta* **2003**, *399*, 203–208.

(14) Bush, M. E.; Bouley, N. D.; Urbach, A. R. Charge-mediated recognition of N-terminal tryptophan in aqueous solution by a synthetic host. *J. Am. Chem. Soc.* **2005**, *127*, 14511–14517.

(15) Rajgariah, P.; Urbach, A. R. Scope of amino acid recognition by cucurbit[8]uril. *J. Inclusion Phenom. Macrocyclic Chem.* **2008**, *62*, 251–254.

(16) Zhang, H.; Grabenauer, M.; Bowers, M. T.; Dearden, D. V. Supramolecular modification of ion chemistry: modulation of peptide charge state and dissociation behavior through complexation with cucurbit[n]uril ( $n = 5, 6$ ) or  $\alpha$ -cyclodextrin. *J. Phys. Chem. A* **2009**, *113*, 1508–1517.

(17) Smith, L. C.; Leach, D. G.; Blaylock, B. E.; Ali, O. A.; Urbach, A. R. Sequence-specific, nanomolar peptide binding via cucurbit[8]uril-induced folding and inclusion of neighboring side chains. *J. Am. Chem. Soc.* **2015**, *137*, 3663–3669.

(18) Li, W.; Bockus, A. T.; Vinciguerra, B.; Isaacs, L.; Urbach, A. R. Predictive recognition of native proteins by cucurbit[7]uril in a complex mixture. *Chem. Commun.* **2016**, *52*, 8537–8540.

(19) (a) Thuéry, P. L-Cysteine as a chiral linker in lanthanide–cucurbit[6]uril one-dimensional assemblies. *Inorg. Chem.* **2011**, *50*, 10558–10560. (b) Gamal-Eldin, M. A.; Macartney, D. H. Selective molecular recognition of methylated lysines and arginines by cucurbit[6]uril and cucurbit[7]uril in aqueous solution. *Org. Biomol. Chem.* **2013**, *11*, 488–495.

(20) Danylyuk, O.; Fedin, V. P. Solid-State Supramolecular Assemblies of Tryptophan and Tryptamine with Cucurbit[6]uril. *Cryst. Growth Des.* **2012**, *12*, 550–555.

(21) Lee, J. W.; Lee, H. H. L.; Ko, Y. H.; Kim, K.; Kim, H. I. Deciphering the Specific High-Affinity Binding of Cucurbit[7]uril to Amino Acids in Water. *J. Phys. Chem. B* **2015**, *119*, 4628–4636.

(22) (a) Heitmann, L. M.; Taylor, A. B.; Hart, P. J.; Urbach, A. R. Sequence-Specific Recognition and Cooperative Dimerization of N-Terminal Aromatic Peptides in Aqueous Solution by a Synthetic Host. *J. Am. Chem. Soc.* **2006**, *128*, 12574–12581. (b) Logsdon, L. A.; Schardon, C. L.; Ramalingam, V.; Kwee, S. K.; Urbach, A. R. Nanomolar Binding of Peptides Containing Noncanonical Amino Acids by a Synthetic Receptor. *J. Am. Chem. Soc.* **2011**, *133*, 17087–17092.

(23) (a) Biedermann, F.; Nau, W. M. Noncovalent chirality sensing ensembles for the detection and reaction monitoring of amino acids, peptides, proteins, and aromatic drugs. *Angew. Chem., Int. Ed.* **2014**, *53*, 5694–5699. (b) Assaf, K. I.; Nau, W. M. Cucurbiturils: from synthesis to high-affinity binding and catalysis. *Chem. Soc. Rev.* **2015**, *44*, 394–418.

(24) Sonzini, S.; Marcozzi, A.; Gubeli, R. J.; van der Walle, C. F.; Ravn, P.; Herrmann, A.; Scherman, O. A. High Affinity Recognition of a Selected Amino Acid Epitope within a Protein by Cucurbit[8]uril Complexation. *Angew. Chem., Int. Ed.* **2016**, *55*, 14000–14004. [10.1002/anie.201606763](https://doi.org/10.1002/anie.201606763); *Angew. Chem.* **2016**, *128*, 14206–14210. [10.1002/ange.201606763](https://doi.org/10.1002/ange.201606763)

(25) Minami, T.; Esipenko, N. A.; Zhang, B.; Isaacs, L.; Anzenbacher, P. “Turn-on” fluorescent sensor array for basic amino acids in water. *Chem. Commun.* **2014**, *50*, 61–63.

(26) Yi, J.-M.; Zhang, Y.-Q.; Cong, H.; Xue, S.-F.; Tao, Z. Crystal structures of four host–guest inclusion complexes of  $\alpha, \alpha', \delta, \delta'$ -

tetramethylcucurbit[6]uril and cucurbit[8]uril with some l-amino acids. *J. Mol. Struct.* **2009**, *933*, 112–117.

(27) Cong, H.; Tao, L.-L.; Yu, Y.-H.; Yang, F.; Du, Y.; Xue, S.-F.; Tao, Z. Molecular recognition of amino acid by cucurbiturils. *Acta Chim. Sin.* **2006**, *64*, 989–996.

(28) Zhang, J.; Xi, Y.-Y.; Li, Q.; Tang, Q.; Wang, R.; Huang, Y.; Tao, Z.; Xue, S.-F.; Lindoy, L. F.; Wei, G. Supramolecular Recognition of Amino Acids by Twisted Cucurbit[14]uril. *Chem.—Asian J.* **2016**, *11*, 2250–2254.

(29) Isaacs, L.; Park, S.-K.; Liu, S.; Ko, Y. H.; Selvapalam, N.; Kim, Y.; Kim, H.; Zavalij, P. Y.; Kim, G.-H.; Lee, H.-S.; Kim, K. The Inverted Cucurbit[n]uril Family. *J. Am. Chem. Soc.* **2005**, *127*, 18000–18001.

(30) Liu, S. M.; Kim, K.; Isaacs, L. Mechanism of the Conversion of Inverted CB[6] to CB[6]. *J. Org. Chem.* **2007**, *72*, 6840.

(31) Pinjari, R. V.; Gejji, S. P. Inverted cucurbit[n]urils: density functional investigations on the electronic structure, electrostatic potential, and NMR chemical shifts. *J. Phys. Chem. A* **2009**, *113*, 1368–1376.

(32) Isaacs, L. D.; Liu, S. M.; Kim, K.; Park, S. K.; Ko, Y. H.; Kim, H.; Kim, Y.; Selvapalam, N. Introverted cucurbituril compounds and their preparation, crystal structure and binding properties. *PCT Int. Appl.* **2007**, 48–51.

(33) Li, Q.; Zhang, Y.-Q.; Zhu, Q.-J.; Xue, S.-F.; Tao, Z.; Xiao, X. Coordination of Alkaline Earth Metal Ions in the Inverted Cucurbit[7]uril Supramolecular Assemblies Formed in the Presence of  $[\text{ZnCl}_4]^{2-}$  and  $[\text{CdCl}_4]^{2-}$ . *Chem.—Asian J.* **2015**, *10*, 1159–1164.

(34) Li, Q.; Qiu, S.-C.; Zhang, Y.-Q.; Xue, S.-F.; Tao, Z.; Prior, T. J.; Redshaw, C.; Zhu, Q.-J.; Xiao, X. Supramolecular assemblies constructed from inverted cucurbit[7]uril and lanthanide cations: synthesis, structure and sorption properties. *RSC Adv.* **2016**, *6*, 77805–77810.

(35) Qiu, S.-C.; Li, Q.; Chen, K.; Zhang, Y.-Q.; Zhu, Q.-J.; Tao, Z. Absorption properties of an inverted cucurbit[7]uril-based porous coordination polymer induced by  $[\text{ZnCl}_4]^{2-}$  anions. *Inorg. Chem. Commun.* **2016**, *72*, 50–53.

(36) Li, Q.; Qiu, S.-C.; Lu, J.-H.; Xue, S.-F.; Xiao, X.; Tao, Z.; Zhu, Q.-J. Host–guest interactions in an inverted cucurbit[7]uril with  $\alpha, \omega$ -alkyldiammonium guests. *RSC Adv.* **2015**, *5*, 68914–68918.

(37) Gao, Z.; Yang, L.; Bai, D.; Chen, L.; Tao, Z.; Xiao, X. Interaction of Inverted Cucurbit[7]uril with N,N'-dibenzyl-4,4'-pyridine Chloride. *Chem. Res. Chin. Univ.* **2017**, *38*, 212–216.

(38) Gao, Z.; Bai, D.; Chen, L.; Tao, Z.; Xiao, X.; Prior, T. J.; Redshaw, C. A study of the interaction between inverted cucurbit[7]uril and symmetric viologens. *RSC Adv.* **2017**, *7*, 461–467.

(39) Mock, W. L.; Shih, N. Y. Structure and selectivity in host–guest complexes of cucurbituril. *J. Org. Chem.* **1986**, *51*, 4440–4446.

(40) Dixit, P. H.; Pinjari, R. V.; Gejji, S. P. Electronic Structure and  $^1\text{H}$  NMR Chemical Shifts in Host–Guest Complexes of Cucurbit[6]uril and sym-Tetramethyl Cucurbit[6]uril with Imidazole Derivatives. *J. Phys. Chem. A* **2010**, *114*, 10906–10916.

(41) Bailey, D. M.; Hennig, A.; Uzunova, V. D.; Nau, W. M. Supramolecular tandem enzyme assays for multiparameter sensor arrays and enantiomeric excess determination of amino acids. *Chem.—Eur. J.* **2008**, *14*, 6069–6077.